



Inhibition of L-Type Ca^{2+} Channels by TRPC1-STIM1 Complex Is Essential for the Protection of Dopaminergic Neurons

Yuyang Sun,¹  Haopeng Zhang,¹ Senthil Selvaraj,¹ Pramod Sukumaran,¹ Saobo Lei,¹ Lutz Birnbaumer,² and  Brij B. Singh¹

¹Department of Biomedical Sciences, School of Medicine and Health Sciences, University of North Dakota, Grand Forks, North Dakota 58201, and ²National Institutes of Environmental Health Sciences, Durham, North Carolina 27709

Loss of dopaminergic (DA) neurons leads to Parkinson's disease; however, the mechanism(s) for the vulnerability of DA neurons is(are) not fully understood. We demonstrate that TRPC1 regulates the L-type Ca^{2+} channel that contributes to the rhythmic activity of adult DA neurons in the substantia nigra region. Store depletion that activates TRPC1, via STIM1, inhibits the frequency and amplitude of the rhythmic activity in DA neurons of wild-type, but not in TRPC1^{-/-}, mice. Similarly, TRPC1^{-/-} substantia nigra neurons showed increased L-type Ca^{2+} currents, decreased stimulation-dependent STIM1- $\text{Ca}_v1.3$ interaction, and decreased DA neurons. L-type Ca^{2+} currents and the open channel probability of $\text{Ca}_v1.3$ channels were also reduced upon TRPC1 activation, whereas increased $\text{Ca}_v1.3$ currents were observed upon STIM1 or TRPC1 silencing. Increased interaction between $\text{Ca}_v1.3$ -TRPC1-STIM1 was observed upon store depletion and the loss of either TRPC1 or STIM1 led to DA cell death, which was prevented by inhibiting L-type Ca^{2+} channels. Neurotoxins that mimic Parkinson's disease increased $\text{Ca}_v1.3$ function, decreased TRPC1 expression, inhibited Tg-mediated STIM1- $\text{Ca}_v1.3$ interaction, and induced caspase activation. Importantly, restoration of TRPC1 expression not only inhibited $\text{Ca}_v1.3$ function but increased cell survival. Together, we provide evidence that TRPC1 suppresses $\text{Ca}_v1.3$ activity by providing an STIM1-based scaffold, which is essential for DA neuron survival.

Key words: calcium; $\text{Ca}_v1.3$; Parkinson's disease; SOCE; TRPC1-STIM1

Significance Statement

Ca^{2+} entry serves critical cellular functions in virtually every cell type, and appropriate regulation of Ca^{2+} in neurons is essential for proper function. In Parkinson's disease, DA neurons are specifically degenerated, but the mechanism is not known. Unlike other neurons, DA neurons depend on $\text{Ca}_v1.3$ channels for their rhythmic activity. Our studies show that, in normal conditions, the pacemaking activity in DA neurons is inhibited by the TRPC1-STIM1 complex. Neurotoxins that mimic Parkinson's disease target TRPC1 expression, which leads to an abnormal increase in $\text{Ca}_v1.3$ activity, thereby causing degeneration of DA neurons. These findings link TRPC1 to $\text{Ca}_v1.3$ regulation and provide important indications about how disrupting Ca^{2+} balance could have a direct implication in the treatment of Parkinson's patients.

Introduction

Parkinson's disease (PD) is a progressive, hypokinetic, neurodegenerative disease. Although the cause of PD is not well under-

stood, it is known that the loss of dopaminergic (DA) neurons in the substantia nigra (SN) region underlies the main motor symptoms for this disease but the mechanism is still not clear. In recent

Received Sept. 26, 2016; revised Feb. 1, 2017; accepted Feb. 16, 2017.

Author contributions: S.L. and B.B.S. designed research; Y.S., H.Z., S.S., S.L., and B.B.S. performed research; Y.S., P.S., L.B., and B.B.S. contributed unpublished reagents/analytic tools; Y.S., H.Z., S.S., P.S., S.L., L.B., and B.B.S. analyzed data; S.S., P.S., and B.B.S. wrote the paper.

This work was supported by National Institutes of Health DE017102, DE024300, and GM113123 to B.B.S., and National Institutes of Health Intramural Research Program Project Z01-ES-101684 to L.B. The confocal facility at University of North Dakota was supported in part by National Institutes of Health COBRE Grant P30GM103329. We thank the United Kingdom Parkinson Society and the Udall Center (Philadelphia) for providing the PD/control samples; and Drs. John Watt and Gunjan Dhawan for assistance.

The authors declare no competing financial interests.

Correspondence should be addressed to Dr. Brij B. Singh, Department of Biomedical Sciences, School of Medicine and Health Sciences, University of North Dakota, Grand Forks, ND 58201. E-mail: brij.singh@med.und.edu.

Present address for L.B.: Institute of Biomedical Research (BIOMED), The Catholic University of Argentina, C1107AFF Buenos Aires, Argentina.

Present address for H.Z.: Department of Anesthesiology, Xijing Hospital, Fourth Military Medical University, Xi'an, Shaanxi Province, PR China.

DOI:10.1523/JNEUROSCI.3010-16.2017

Copyright © 2017 the authors 0270-6474/17/373364-14\$15.00/0

years, attention has turned to the role of calcium (Ca²⁺) in the onset of PD. Ca²⁺-induced excitotoxicity has been considered an important mechanism leading to DA neuron cell death. However, not all of the DA midbrain neurons are equally affected by the degenerative process in PD. In particular, SN DA neurons are highly vulnerable to being affected via environmental factors and toxins that lead to PD compared with more resistant neighboring VTA DA neurons (Björklund and Dunnett, 2007; Dragicevic et al., 2015). It has been proposed that sodium channels play a major role in the spike generation of VTA DA cells, whereas Ca²⁺ channels could contribute to the pacemaking activity in SN DA neurons.

L-type Ca²⁺ channels, mainly Ca_v1.3, have been shown to contribute to the rhythmic activity of DA neurons in the SN region and could render DA neurons susceptible to mitochondrial toxins (Guzman et al., 2010; Surmeier et al., 2011; Dryanovski et al., 2013). Importantly, an increase in Ca_v1.3 expression was observed in PD brains, which precedes PD pathology (Hurley et al., 2015). In addition, a change in the ratio of Ca_v1.2 versus Ca_v1.3 was observed that could contribute to Ca²⁺-mediated excitotoxicity (Guzman et al., 2010; Kang et al., 2012; Hurley et al., 2015). Consistent with these studies, patients treated with Ca_v1 antagonists had a decreased risk for PD (Ritz et al., 2010; Marras et al., 2012). However, in PD, not all DA neurons degenerate and most neurons start to degenerate at the later stage of life, suggesting that there could be alternative mechanisms that may inhibit Ca_v1.3 activity and help in the survival of DA neurons.

Changes in Ca²⁺ homeostasis with regard to storage organelles, such as the ER and mitochondria, have also been shown to affect neuronal survival and are closely linked with PD (Kazuno et al., 2006). Ca²⁺ entry through the store-operated Ca²⁺ entry (SOCE) channels is essential for maintaining intracellular Ca²⁺ stores thus could regulate neuronal function and survival (Bollimuntha et al., 2006; Selvaraj et al., 2012). TRPC1 has been suggested as a candidate for SOCE-mediated Ca²⁺ entry and has been shown to be critical for neuronal survival (Wang and Poo, 2005; Bollimuntha et al., 2006; Selvaraj et al., 2012). In addition, stromal interacting molecule-1 (STIM1) has been identified as the primary regulator of SOCE-mediated Ca²⁺ entry, and store depletion allows STIM1 rearrangement followed by its interaction with TRPC1 that induces Ca²⁺ entry (Huang et al., 2006; Pani et al., 2012). Interestingly, STIM1 has also been shown to inhibit L-type Ca²⁺ channels (Park et al., 2010; Wang et al., 2010); however, the mechanism as to how STIM1 inhibits L-type Ca²⁺ channels is not known. Furthermore, a role for SOCE-mediated Ca²⁺ entry in the regulation of Ca_v1.3 channels in DA neurons has yet to be established. Thus, the objective of this study was to identify the relationship between TRPC1 and Ca_v1.3 channels and establish their role in regulating DA neuronal function. Our previous studies have shown that TRPC1 channels are important for DA neuronal function and protect against cytotoxicity induced by neurotoxins by inhibiting ER stress (Selvaraj et al., 2009, 2012). Results presented here indicate, for the first time, that TRPC1 is essential for the inhibition of L-type Ca²⁺ channels. DA neurons in TRPC1^{-/-} mice showed increased spontaneous rhythmic activity as well as increased degeneration of DA neurons. Furthermore, the frequency of neuronal firing was increased in DA neurons of TRPC1^{-/-} mice and TRPC1-inhibited L-type Ca²⁺ channel, especially Ca_v1.3 activity, by facilitating an STIM1-Ca_v1.3 interaction, which was essential for the protection of DA neurons.

Materials and Methods

Cell culture, transfections, and viability assays. SH-SY5Y cells were obtained from the ATCC and cultured/maintained at 37°C with 95% humidified air and 5% CO₂ and differentiated as previously described (Bollimuntha et al., 2005; Selvaraj et al., 2012). For transient transfection, SH-SY5Y cells were transfected with TRPC1siRNA (Ambion) or Cav1.3 siRNA or STIM1siRNA or scrambled control siRNA (Ambion negative control siRNA #1) using HiPerfect transfection reagent (QIAGEN). For rescue experiments, cells were transfected with siSTIM1 for 24 h followed by overexpression of full-length STIM1 (10-fold concentration). For viability assays, cells were seeded in 96-well plates at a density of 0.5 × 10⁵ cells/well. The cultures were grown for 24 h under different conditions, and cell viability was measured by using the MTT method as described previously (Selvaraj et al., 2012).

Animals and human brain samples. Two- to 5-week-old male C57BL/6 (Charles River) or TRPC1^{-/-} mice were used for these experiments. The TRPC1^{-/-} mice were generated as previously described (Liu et al., 2007). All animals were housed in a temperature-controlled room under a 12/12 h light/dark cycle with *ad libitum* access to food and water, and experiments were performed as per the institutional guidelines for the use and care of animals. Frozen and paraffin-embedded blocks of post-mortem human SN samples of control (6 samples, males with age ranging from 65 to 72 years) and PD patients (8 samples, males and females with age ranging from 60 to 72 years, with severe motor neuron deficit) were obtained from United Kingdom Parkinson's foundation as well as Udall Parkinson Center (Philadelphia). All human subjects were approved by the institutional review board. Immunofluorescence was performed on sections using specific antibodies as described.

Brain slice preparation and electrophysiology. Mice (2–5 weeks old) were killed, and the brain was dissected in ice-cold saline solution. Coronal brain sections (400 μm) were cut using a vibrating blade microtome (VT1000S; Leica). Brain slice recordings were performed under infrared videomicroscopy (Olympus BX51WI) as described previously (Zhang et al., 2014). Recording electrodes were filled with (in mM) as follows: 100 K⁺-gluconate, 0.6 EGTA, 2 MgCl₂, 8 NaCl, 33 HEPES, 2 ATPNa₂, 0.4 GTPNa, and 7 phosphocreatine, pH 7.4. The extracellular solution comprised the following (in mM): 130 NaCl, 24 NaHCO₃, 3.5 KCl, 1.25 NaH₂PO₄, 2.5 CaCl₂, 1.5 MgCl₂, and 10 glucose, saturated with 95% O₂ and 5% CO₂, pH 7.4. For calcium current recordings, TTX is added in the extracellular solution and K⁺-gluconate is replaced with CsCl in intracellular solution. For SOCE current recordings, recording electrodes were filled with the following (in mM): 110 CsCl, 5 MgCl₂, 10 EGTA, 10 HEPES, 4 ATPNa₂, and 0.1 GTPNa, pH 7.4. Treatments applied after the firing had been stable for 5–10 min. Amplitude and frequency were calculated by Mini Analysis 6.0.1 (Synaptosoft). For Ca²⁺ currents, cells were voltage-clamped using a train of three action potentials (APs) that showed spontaneous firing and was used to establish the time course of Ca²⁺ currents under AP trains (Marcantoni et al., 2010; Vandael et al., 2012). For single-cell recordings, coverslips with SH-SY5Y cells were transferred to the recording chamber and perfused with an external Ringer's solution of the following composition (mM): 125 TEA-Cl, 10 CaCl₂, 10 HEPES, 10 glucose, pH 7.4 (Tris). The patch pipette was filled with the standard intracellular solution that contained the following (mM): 130 CsCl, 2 MgCl₂, 20 HEPES, 11 EGTA, 2 Na₂ATP, 0.1 GTP, 10 glucose, pH 7.3 (CsOH). All electrophysiological experiments were filtered at 2 kHz, digitized at 10 kHz, and acquired and analyzed using pCLAMP 10 software (Molecular Devices). All experiments were performed at room temperature.

Single-channel recording. For single-channel recording in cell-attached configuration, recording electrodes were filled with the following (in mM): 100 TEA-Cl, 10 BaCl₂, 10 HEPES, pH 7.4 (Tris). The extracellular solution used to set the membrane potential to zero comprised of the following (in mM): 104 K-aspartate, 1 MgCl₂, 10 HEPES, 10 EGTA, pH 7.4. Data were obtained in response to membrane depolarizing pulse, 200 ms duration, from an intracellular holding -40 mV, filtered at 2 kHz, digitized at 10 kHz, and acquired and analyzed using pCLAMP10 software (Molecular Devices). A threshold level was set at one-half of the estimated unitary current amplitude. The low-variance analysis was used

to estimate single-channel current levels. Briefly, the mean current amplitude and variance were calculated for a window advanced across the record in 1 point increments. If the variance in the window was below the baseline variance, the mean current amplitude was kept for the histogram. The histogram bin width was 0.05 pA for all experiments. All experiments were performed at room temperature.

Calcium measurement. Cells were incubated with 2 μ M fura-2 (Invitrogen) for 45 min and washed twice with Ca^{2+} free standard external solution, including the following: 10 mM HEPES, 120 mM NaCl, 5.4 mM KCl, 1 mM $MgCl_2$, 10 mM glucose, pH 7.4, buffer. For fluorescence measurements, the fluorescence intensity of fura-2-loaded control cells was monitored with a CCD camera-based imaging system (Compix). A monochromator dual-wavelength enabled alternative excitation at 340 and 380 nm, whereas the emission fluorescence was monitored at 510 nm. The images of multiple cells collected at each excitation wavelength were processed using the C imaging, PCI software (Compix), to provide ratios of fura-2 fluorescence from excitation at 340 nm to that from excitation at 380 nm (F340/F380).

Immunofluorescence and immunohistochemistry. Animals were anesthetized and fixed by perfusion with PBS followed by PFA (4%, w/v) in PBS. The whole brain was removed and fixed again overnight in PFA (3%), cryoprotected in 30% sucrose in PBS for 24 h at 4°C, and then frozen in OCT freezing compound (Ted Pella). Serial cryosections were collected through the entire midbrain (10 μ M) and stained using TH-specific antibodies. Secondary antibodies that were conjugated with a fluorophore were used to label individual protein; samples without primary antibody were used as a control. For immunohistochemistry, the Vector ABC Elite kit (Vector Laboratories) was used along with 3'3' diaminobenzoic acid as a chromogen to develop the reaction in the presence of H_2O_2 (Selvaraj et al., 2009). All samples were examined and images obtained using a Leica and Zeiss Meta confocal microscope. For quantitative measurements, persons blind to the treatment counted the number of TH-positive neurons in the SN pars compacta. Measurements from four to six sections per brain were averaged to obtain one value per subject.

Immunoprecipitation and Western blot analysis. Rabbit polyclonal Ab anti-TRPC1 (catalog #ACC-010), anti-TRPC3 (catalog #ACC-016), anti-Orai1, and anti- $Ca_v1.3$ (catalog #ACC-005) were purchased from Alomone Labs. Goat polyclonal Ab against β -actin (catalog #sc-1616) was obtained from Santa Cruz Biotechnology. Rabbit monoclonal Ab against STIM1 (catalog #4916), cleaved caspase3 (catalog #9664), Bak (catalog #2772), and Bid (catalog #2002) were purchased from Cell Signaling Technology. Cells or SN tissues were stimulated (with and without Tg 2 μ M) as indicated in the figure followed by the addition of RIPA buffer to obtain cell lysates from both differentiated SH-SY5Y cells and SN region of the brain. Protein concentrations were determined using the Bradford reagent (Bio-Rad); 25 μ g of lysates was resolved on NuPAGE 4%–12% Bis-Tris gels (Invitrogen) and followed by Western blotting as described previously (Bollimuntha et al., 2005; Selvaraj et al., 2009). For immunoprecipitation, 1 mg of total lysate was incubated overnight (4°C) with the primary antibody, followed by the addition of protein A beads for 3 h, washed with high salt buffer, and resolved on the gel.

Intrastantia nigral injection. Mice received a unilateral injection of either control virus (Ad-GFP) or Ad-TRPC1 (3×10^7 particles per construct in 3 μ l) into the SN. After 1 week of adenovirus injection, mice were challenged with MPTP (MPTP-HCl 25 mg/kg per injection for 5 consecutive days at 24 h intervals). After additional 2 weeks, the brain was removed from the skull and placed dorsal side up. Using a scalpel blade, a coronal cut was made adjacent to the inferior colliculi at bregma ~ -6.36 mm. A second cut was made at bregma ~ -2.54 mm, based on the mouse brain atlas. The ventral midbrain was dissected to ensure that there was no contamination of the hippocampus, cortex, or cerebellum. Brain regions from 2 or 3 animals were pooled for each experiment.

Statistical analysis. Data analysis was performed using Origin 9.0 (OriginLab). Student's paired or unpaired *t* test or ANOVA was used for statistical analysis as appropriate; *N* indicates the cells or slices examined.

Differences in the mean values (mean \pm SEM) were considered to be significant at *p* < 0.05.

Results

L-type Ca^{2+} channel contributes to the rhythmic activity of DA neurons in the SN region

The loss of DA neurons in the SN region is a prominent characteristic of PD. Thus, we analyzed the expression of the dopamine transporter (DAT), which is a marker for dopaminergic neurons in control and PD samples. Importantly, expression of DAT protein was decreased in human PD patients (Fig. 1A,B). Furthermore, most of the DAT staining in PD patients coincided with endocytic vesicular staining, suggesting that DA neurons are affected in PD. However, as both DA and GABAergic neurons are present in the SN region that modulates dopamine release and function, electrophysiological experiments were performed in slices obtained from SN region of adults (*p* > 28 d) mice. In the whole-cell configuration, the mean frequency of spontaneous APs in GABAergic neurons was much higher than that observed in DA neurons (Fig. 1C,E). Hyperpolarizing current pulses of 200 pA were also used to distinguish between the two neuronal populations, and APs evoked by current injection showed distinct characteristics between the DA and GABAergic neurons (Matsuda et al., 1987; Yung et al., 1991; Richards et al., 1997; Seutin and Engel, 2010) (Fig. 1D,F). Additionally, consistent with previous reports (Okamoto et al., 2006), DA neurons, exhibited I_h ratio < 0.6, whereas GABAergic neurons showed a small I_h (I_h ratio > 0.6) (Fig. 1G–I), in accordance with the presence of the two different types of neurons in the SN region.

One of the fundamental questions that need to be addressed is why distinctively DA neurons are vulnerable in PD. Interestingly, most neurons exhibit exclusively TTX (a Na^+ channel inhibitor) sensitive autonomous pacemakers; however, in the SN area, DA neurons have shown to be partially dependent on Ca^{2+} for its autonomous pacemaking activity (Surmeier et al., 2011). To study this further, tissue slices from the adult SN area were used and AP activity was recorded. As shown in Figure 2A, B, the addition of TTX completely blocked the rhythmic activity in GABAergic neurons. Similar results were also observed in juvenile (P14–P18 d) DA neurons (Fig. 2C,D), which showed that TTX was also able to block the rhythmic activity in DA neurons. In contrast, the rhythmic activity of aged DA neurons (*p* > 28 d) was only partially decreased by the addition of TTX (Fig. 2E,F). In addition, 20% of cells showed slow oscillatory potentials upon application of TTX (Fig. 2G). Furthermore, the rhythmic activity was facilitated by the application of Bay K8644 (L-type Ca^{2+} channel activator) (Fig. 2H). The addition of nifedipine (an L-type Ca^{2+} channel blocker) along with TTX completely abolished the rhythmic activity of aged DA neurons (Fig. 2I). Importantly, removal of external Ca^{2+} completely inhibited the TTX-resistant rhythmic activity in adult DA neurons (Fig. 2J). Together, these results suggest that the rhythmic activity in aged DA neurons is in part driven by the L-type Ca^{2+} channels. In neurons, L-type Ca^{2+} channels have one of the two $\alpha 1$ -subunits: $Ca_v1.2$ or $Ca_v1.3$. The $Ca_v1.3$ subunits are highly expressed in the SN region and open at relatively hyperpolarized potentials (Koschak et al., 2001; Xu and Lipscombe, 2001; Helton et al., 2005; Chan et al., 2007; Surmeier et al., 2011; Hurley et al., 2015). Together, these data suggest that the contribution of L-type Ca^{2+} channels, especially $Ca_v1.3$, could play a key role in DA neuron vulnerability and degeneration.

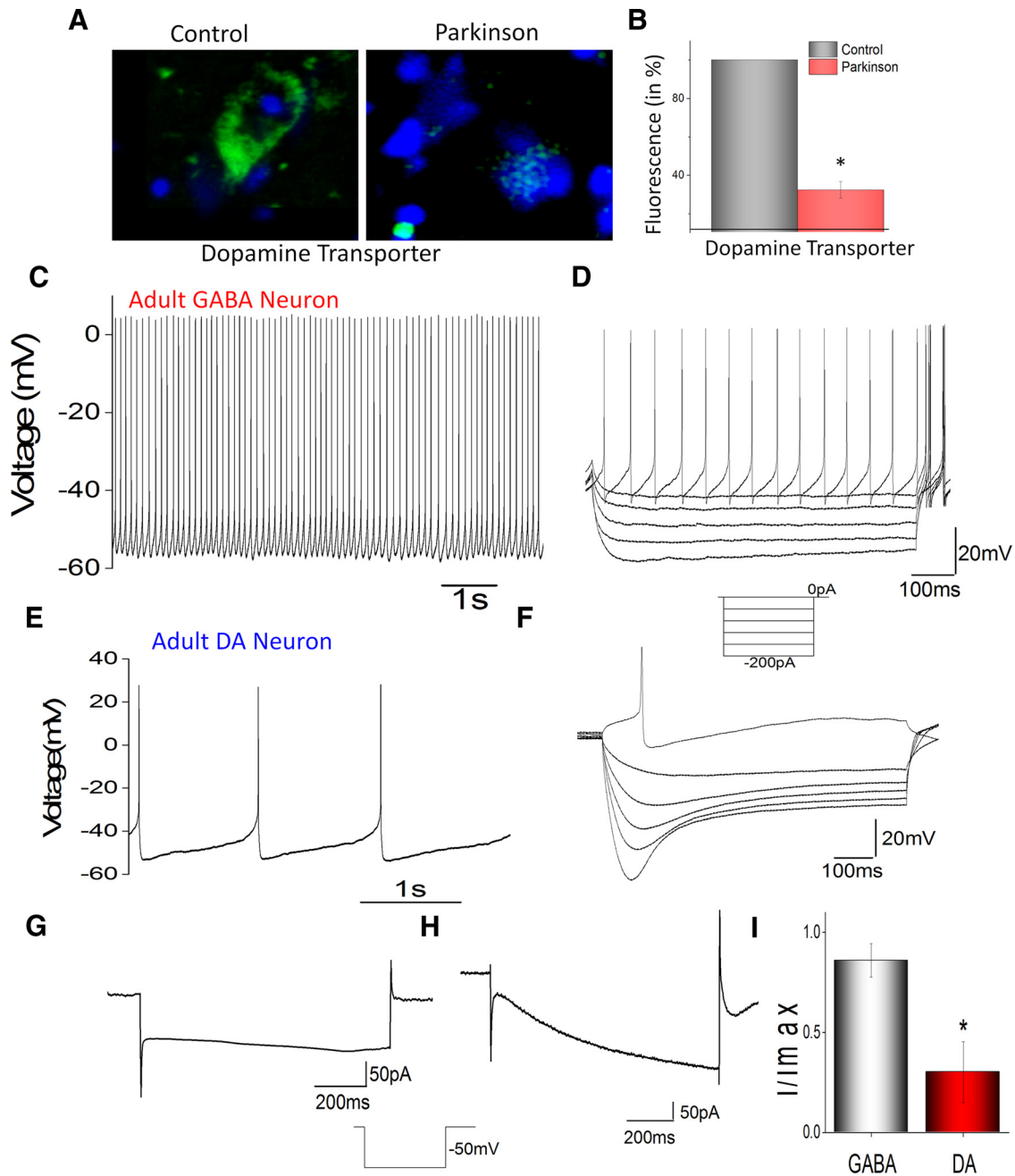


Figure 1. Functional characterization of DA and GABAergic neurons in the SN region. **A**, Paraffin-embedded sections of postmortem human SN region obtained from control and PD patients. Sections were immunostained using DAT. **B**, Quantification of the fluorescence obtained from 5 or 6 individual sections. Patterns of AP firing using tissue slices from SN area in a GABA neuron (**C**) and in adult DA neurons (**E**). Traces were recorded without current injection. **D**, **F**, Voltage traces were evoked by a series of 1000 ms current pulses (from -200 pA with increment -40 pA). **G**, **H**, Current traces evoked by -50 mV steps from holding potential -60 mV. **I**, Bar graph represents I_h ratio in GABA and DA neurons ($n = 15$). * $p < 0.05$.

TRPC1 inhibits the rhythmic activity of DA neurons in the SN area

Our previous studies had shown that another Ca^{2+} channel, TRPC1, is also involved in regulating Ca^{2+} homeostasis and protects against the loss of DA neurons (Bollimuntha et al., 2005; Selvaraj et al., 2012). Thus, given the importance of Ca^{2+} for the rhythmic activity in DA neurons, we further investigated the relationship between L-type Ca^{2+} channels and TRPC1 in aged DA neurons ($p > 28$ d). The spontaneous activity of DA neurons was recorded under the current-clamp mode. Interestingly, tissue slices from SN region of $TRPC1^{-/-}$ mice showed an increase in the AP (1.02 ± 0.07 Hz, $n = 9$) compared with age-matched

wild-type control mice (0.80 ± 0.04 Hz, $n = 9$) (Fig. 3A,E), suggesting that loss of TRPC1 increases the rhythmic activity of the DA neurons. To further confirm this, TTX was added; and although TTX decreased the rhythmic activity of DA neurons in wild-type mice and $TRPC1^{-/-}$ mice, the rhythmic activity in $TRPC1^{-/-}$ mice (0.41 ± 0.03 Hz, $n = 9$) was slightly higher compared with wild-type DA neurons (0.35 ± 0.04 Hz, $n = 9$) treated with TTX (Fig. 3B,F,M). The addition of nifedipine, which blocks L-type Ca^{2+} channels, inhibited the pacemaking activity in both wild-type and $TRPC1^{-/-}$ mice (data not shown). More importantly, application of thapsigargin (Tg, a SERCA pump blocker, which activates TRPC1 channels) (Liu et al., 2003;

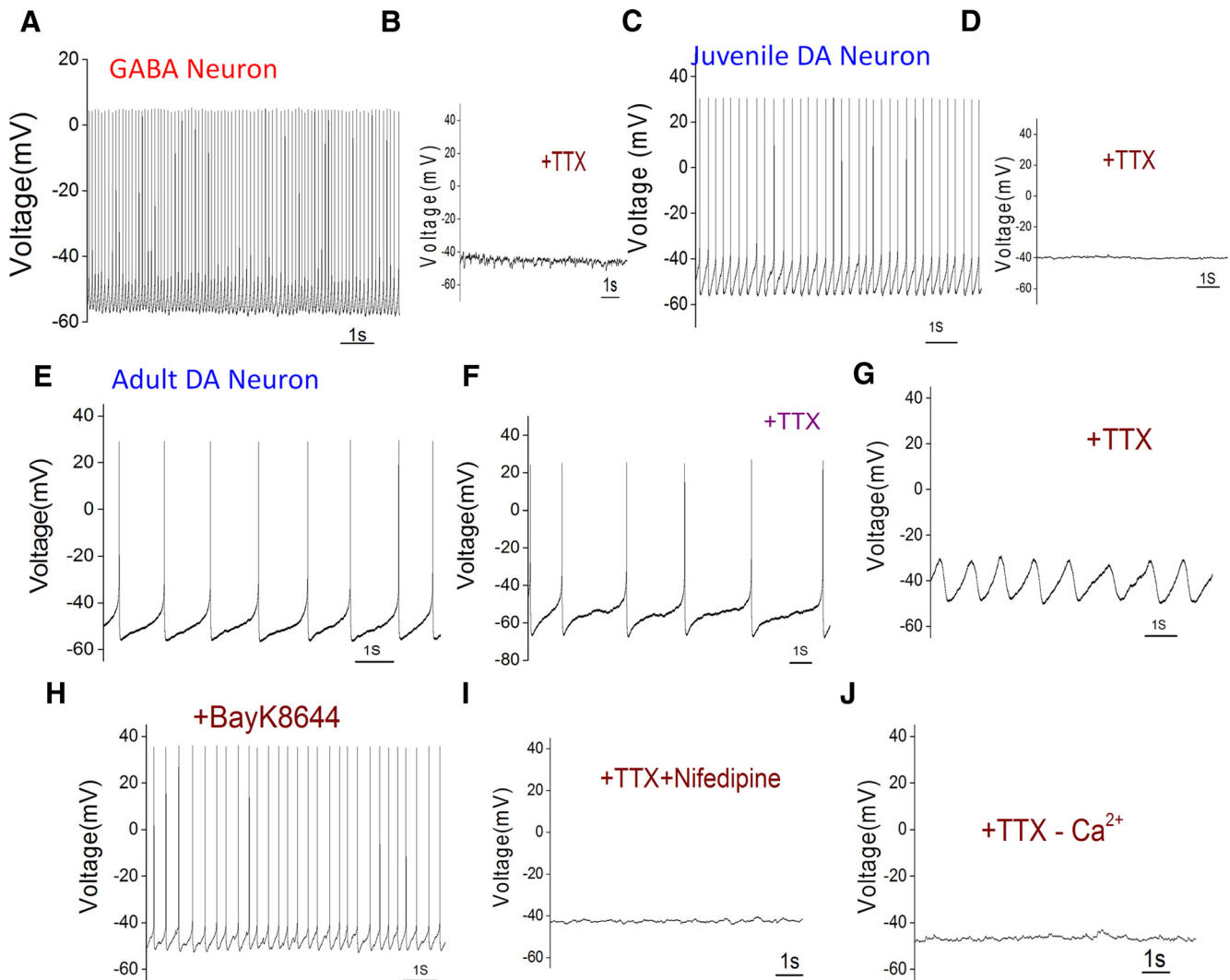


Figure 2. $Ca_v1.3$ channels contribute to the rhythmic activity of DA neurons. In the whole-cell configuration, application of $0.5 \mu\text{M}$ TTX abolished spiking of GABA neurons in wild-type mice (**A, B**). **C**, Spontaneous APs and application of $0.5 \mu\text{M}$ TTX abolished spiking of DA neurons in juvenile mice (P14–P18 d) (**D**). **E**, Patterns of AP firing in adult ($p > 28$ d) DA neurons from the SN area. **F, G**, Application of $0.5 \mu\text{M}$ TTX decreased spiking in adult DA neurons. **H**, Application of $1 \mu\text{M}$ BayK8644 increased spiking. **I**, The addition of $1 \mu\text{M}$ nifedipine abolished spiking of DA neurons in adult mice. **J**, Application of $0.5 \mu\text{M}$ TTX along with removing external Ca^{2+} also abolished spiking of DA neurons in adult mice.

Selvaraj et al., 2012) along with TTX significantly inhibited both the frequency (0.21 ± 0.05 Hz, $n = 8$) and the amplitude of rhythmic activity of DA neurons in wild-type mice (Fig. 3C, I, N). In contrast, the activity of DA neurons in $TRPC1^{-/-}$ mice was not affected, and no decrease in the frequency (0.38 ± 0.04 Hz, $n = 8$) or amplitude of the rhythmic activity was observed by the addition of Tg along with TTX (Fig. 3G, J, N). Application of 2-APB (a nonspecific TRPC1 blocker) abolished the effect of Tg-mediated decrease in rhythmic activity in wild-type mice (Fig. 3D, K) (0.35 ± 0.06 Hz, $n = 6$) but showed no decrease in the rhythmic activity in $TRPC1^{-/-}$ mice (0.40 ± 0.06 Hz, $n = 6$) (Fig. 3H, L). These results further establish that activation of TRPC1 inhibits spontaneous pacemaking activity in DA neurons.

L-type Ca^{2+} channel activity in the SN region is inhibited by TRPC1

The results shown above suggest that, in DA neurons, TRPC1 inhibits the autonomous activity driven by L-type VGCCs. To confirm that functional TRPC1 channels exist in DA neurons, we stimulated DA neurons with Tg to measure SOCE currents. As indicated in Figure 4A, B, store depletion induced an inward

TRPC1-like current in WT DA neurons, and the current properties were similar as previously reported (Liu et al., 2003; Selvaraj et al., 2012). The addition of 2-APB or knockdown of TRPC1 ($TRPC1^{-/-}$) significantly inhibited SOCE currents that were induced by store depletion (Fig. 4A–C), suggesting that TRPC1 channel functions as a putative SOCE channel in DA neurons. To further confirm the role of TRPC1 in regulating VGCC, we next recorded the Ca^{2+} currents in the tissue slices from the SN area. Importantly, the VGCC activity in $TRPC1^{-/-}$ mice was increased compared with wild-type control mice. Moreover, store depletion, by the addition of Tg, significantly decreased Ca^{2+} currents in wild-type mice, whereas no such decrease in the VGCC activity was observed in $TRPC1^{-/-}$ mice (Fig. 4D–G). The addition of nifedipine was able to block the Ca^{2+} currents in the SN region of wild-type and $TRPC1^{-/-}$ mice (Fig. 4D–F). Similarly, under physiological conditions, VGCC-mediated Ca^{2+} currents were also significantly increased in $TRPC1^{-/-}$ mice compared with wild-type (Fig. 4H, I). Moreover, overload of calcium further increased VGCC-mediated Ca^{2+} currents in $TRPC1^{-/-}$ mice (data not shown). Importantly, no change in the expression of $Ca_v1.3$ or STIM1 or Orai1 was observed in $TRPC1^{-/-}$ mice (Fig.

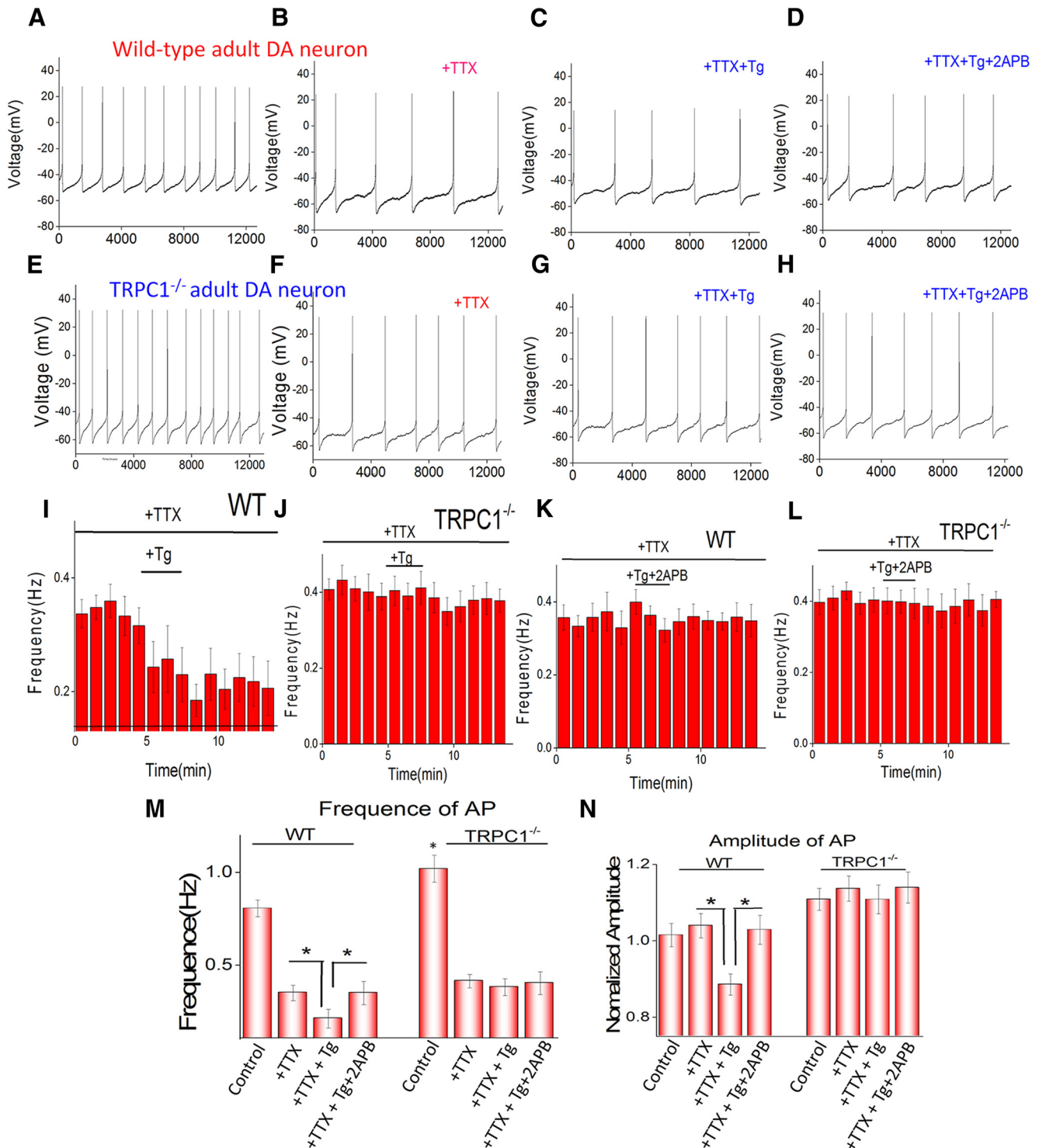


Figure 3. TRPC1 inhibits the rhythmic activity of DA neurons in the SN region. In the whole-cell configuration, patterns of AP firing of adult DA neurons ($p > 28$ d) in wild-type mice (**A**) and $TRPC1^{-/-}$ mice (**E**). **B, F**, AP firing upon application of $0.5 \mu\text{M}$ TTX in both wild-type and $TRPC1^{-/-}$ slices. **C, G**, Rhythmic activity in SN slices that were incubated with $1 \mu\text{M}$ Tg + TTX in wild-type and $TRPC1^{-/-}$ mice, respectively. **D, H**, Rhythmic activity in SN slices that were incubated with $1 \mu\text{M}$ Tg + TTX + $50 \mu\text{M}$ APB in wild-type and $TRPC1^{-/-}$ mice, respectively. **I–L**, Pooled time course of AP firing frequency under various conditions in WT and $TRPC1^{-/-}$ mice ($n = 9$). **M, N**, The frequencies and normalized amplitude under these conditions. *Significantly different values ($p < 0.05$) ($n = 9$).

4J, K), suggesting that alterations in Ca²⁺ currents are specifically dependent on TRPC1 expression.

Recent findings have shown that store depletion induces STIM1 aggregation and increases STIM1 interaction with TRPC1, thus activating TRPC1 channels (Huang et al., 2006) that could suppress L-type Ca²⁺ channel currents. These findings led

us to test whether the TRPC1-STIM1 complex interacts with Ca_v1.3. Application of $1 \mu\text{M}$ Tg showed an increase in the pull-down of Ca_v1.3 by STIM1 in wild-type mice compared with unstimulated conditions (Fig. 5A). However, in $TRPC1^{-/-}$ mice, the store-dependent increase in the STIM1-Ca_v1.3 association was abolished, suggesting that STIM1 interaction with Ca_v1.3 is

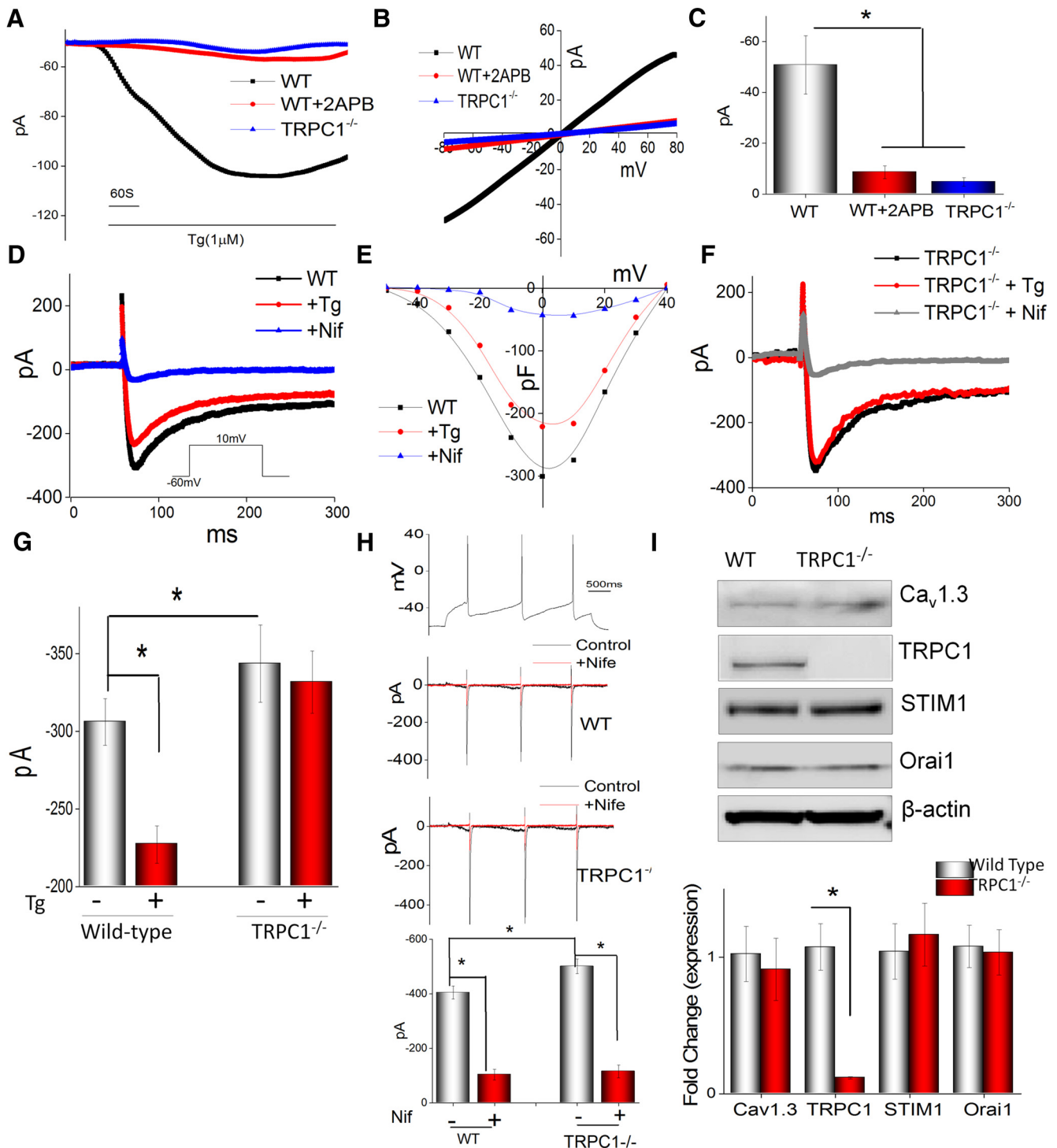


Figure 4. TRPC1 modulates $Ca_v1.3$ activity in SN area of mice. **A**, Representative trace showing store dependent (upon addition of $1 \mu M$ Tg Ca^{2+} entry at -70 mV holding potential) that induced a TRPC1-like current in DA neurons of WT mice but was abolished in the $TRPC1^{-/-}$ mice. Application $50 \mu M$ 2-APB also significantly inhibited the currents in wild-type mice. **B**, $I-V$ curves under these conditions. **C**, Maximum current (at -70 mV holding potential) in wild-type with and without 2-APB and in $TRPC1^{-/-}$ mice ($n = 11$). **D**, Representative trace showed that calcium currents evoked in DA neurons from SN area using a step protocol from -60 to 10 mV in the whole-cell configuration in wild-type mice. **E**, Representative $I-V$ relations under these conditions ($n = 8$). **F**, Representative trace showed that Ca^{2+} currents evoked in DA neurons from SN area in $TRPC1^{-/-}$ mice. **G**, The average ($10-12$ recordings) currents under various conditions ($n = 10$). * $p < 0.05$. **H**, A train of three APs induced Ca^{2+} currents in WT and $TRPC1^{-/-}$ mice ($n = 5$). * $p < 0.05$. **I**, Western blots of lysates from SN tissues from control and $TRPC1^{-/-}$ mice. Antibodies used are indicated in the figure. Densitometry for normalized $Ca_v1.3$ relative to β -actin bar graph is to show quantitation from at least three independent experiments. Data are mean \pm SEM from three independent experiments. * $p < 0.05$.

dependent on TRPC1 expression. To establish the importance of TRPC1 in DA neurons, we next investigated the presence of DA neurons in the SN area by evaluating the TH expression in wild-type and $TRPC1^{-/-}$ mice from the mid region (rostral to

caudal). Interestingly, TH-positive neurons showed that DA neurons in the SN region were significantly decreased in $TRPC1^{-/-}$ mice compared with the wild-type mice. In contrast, DA neurons present in the VTA region showed no such

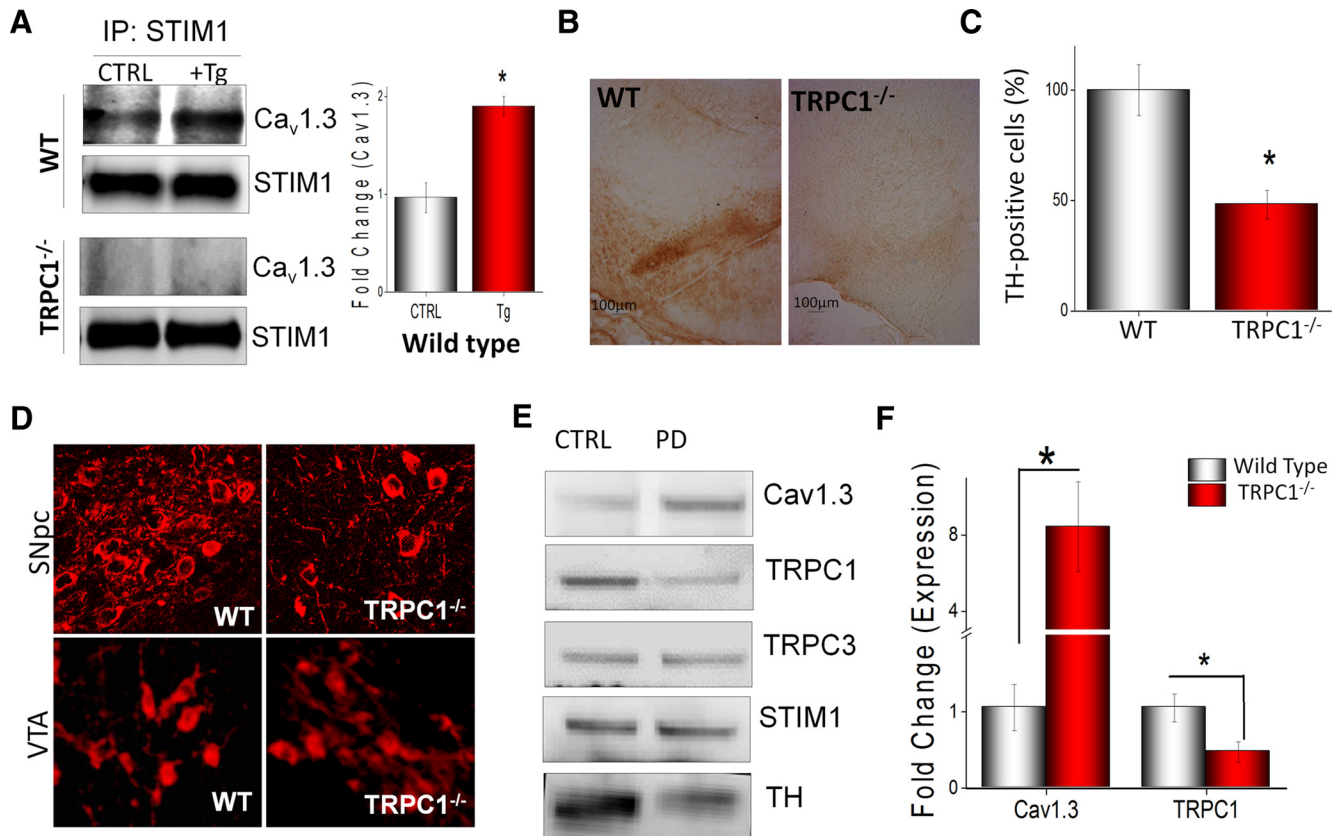


Figure 5. TRPC1 provides a STIM1 scaffold that protects TH-positive neurons in SN region. **A**, Western blots of coimmunoprecipitates of SN tissues using STIM1 antibody under control (CTRL) and stimulated (store depletion, +Tg) conditions. Bar graph represents densitometry for fold change in $Ca_v1.3$ pull-down to show quantitation from at least three independent experiments. **B**, Representative DAB images of brain sections showing full SN region stained with TH antibody from wild-type and TRPC1^{-/-} mice. **C**, Bar graph represents stereology of TH staining from rostral to the caudal region. Data are mean \pm SE. *Significantly different values ($p < 0.05$). $n = 4$. **D**, Immunostaining of TH cells in SN and VTA region obtained from wild-type and TRPC1^{-/-} mice. **E**, Western blots of lysates from SN tissues from control and PD samples. Antibodies used are labeled in the figure. **F**, Densitometric quantitation for normalized TRPC1 or $Ca_v1.3$ relative to TH expression. Data are mean \pm SEM from three independent experiments. * $p < 0.05$.

decrease in TH staining, indicating that loss of TRPC1 renders SN region DA neurons more vulnerable (Fig. 5B–D). Consistent with these results, PD samples also showed a decrease in TH and TRPC1 expression without any change in STIM1 and TRPC3 expression, whereas an increase in $Ca_v1.3$ channels was observed (Fig. 5E,F). Collectively, these results indicate that inhibition of VGCC channels by TRPC1 (providing the scaffold to allow STIM1-mediated inhibition) may be the checkpoint responsible for protecting DA neurons in the SN region and loss of TRPC1.

TRPC1-STIM1 complex regulates $Ca_v1.3$ function

To further confirm the role of TRPC1 and STIM1 in regulating VGCC, we used differentiated SH-SY5Y neuroblastoma cells and evaluated SOCE activity in these cells. Importantly, store depletion (addition of Tg) showed a robust increase in the Ca^{2+} entry (SOCE) in control cells, which was significantly decreased in TRPC1-silenced cells (Fig. 6A). TRPC1 protein levels were also decreased in TRPC1-silenced cells (Fig. 6A). In addition, whole-cell recordings for VGCC were also performed, and knockdown of TRPC1 significantly facilitated VGCC activity without changing the $I-V$ relationship (Fig. 6B,C,K). Importantly, no change in the inactivation of the VGCC currents was observed in TRPC1 silenced cells (Fig. 6D). Both the pore-forming $\alpha 1$ -subunits of VGCC, $Ca_v1.2$, and $Ca_v1.3$ are expressed in DA cells (Sinnegger-Brauns et al., 2009; Kang et al., 2012) and are inhibited by nifedipine. To distinguish which channel is mediated by the

pharmacological effect of nifedipine in DA cells, we silenced $Ca_v1.3$ in differentiated SH-SY5Y cells. Notably, si $Ca_v1.3$ decreased VGCC activity and abolished the effect of siTRPC1 on Ca^{2+} currents, indicating that TRPC1 modulates $Ca_v1.3$ activity (Fig. 6E,F). Similar results were also obtained with STIM1 silencing where decreased expression of STIM1 not only decreased STIM1 levels but also potentiated $Ca_v1.3$ activity (Fig. 6G,H). In addition, STIM1 silencing decreased store-mediated Ca^{2+} entry in SH-SY5Y cells, whereas restoration of STIM1 expression in STIM1 silenced cells (rescue) was able to restore STIM1 expression as well as store-mediated Ca^{2+} entry (Fig. 6I,J).

To establish the mechanism as to how TRPC1 modulates VGCC, we performed single-channel analysis in control and stimulated conditions (store depletion). Importantly, an increase in the single-channel activity of the L-type Ca^{2+} currents was observed, which was inhibited by the addition of nifedipine (Fig. 7A,B). Importantly, store depletion also showed a decrease in the single-channel activity of the L-type Ca^{2+} currents (Fig. 7A,C). Finally, silencing of $Ca_v1.3$ in these cells confirmed that these currents are mediated via the L-type Ca^{2+} channels, and store depletion along with silencing does not further decrease these currents (Fig. 7D,E). As TRPC1 is active upon store depletion, these results suggest that activation of TRPC1 increases STIM1 interaction with VGCC to decrease VGCC activity. To further confirm these results, we tested whether these proteins physically interact in SH-SY5Y cells. Consistent with the *in vivo* studies, immunoprecipitation using STIM1 antibodies resulted in coim-

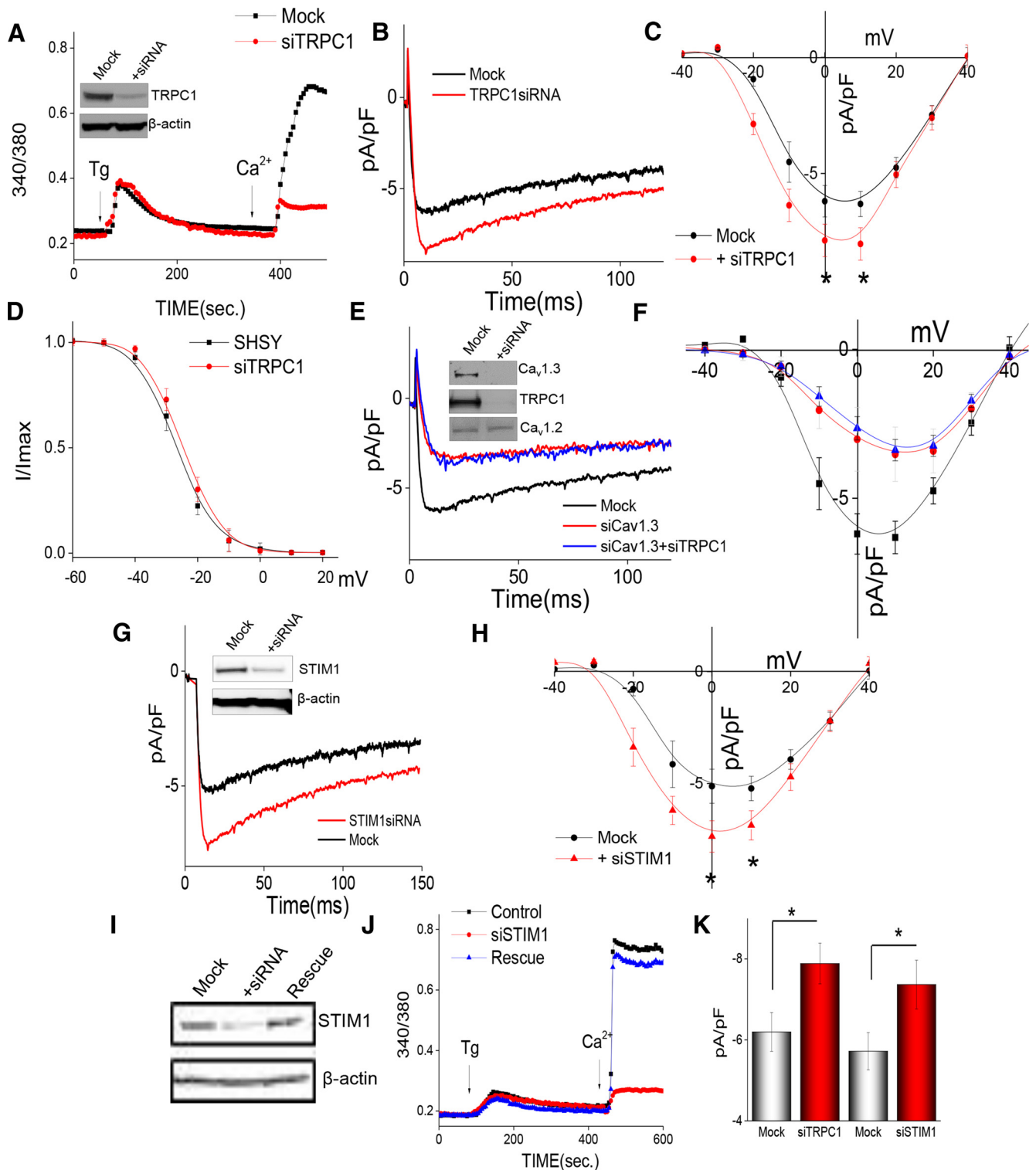


Figure 6. $Ca_v1.3$ channel activity in SH-SY5Y cells is regulated via TRPC1-STIM1. Representative Ca^{2+} traces in differentiated SH-SY5Y cells showed that silencing of STIM1 significantly inhibited Ca^{2+} influx that was induced upon store depletion (+ 1 μ M Tg) (A). STIM1 or TRPC1 silencing increases L-type calcium currents (B and G, respectively). The average (8–10 recordings) $I-V$ relations under these conditions are shown in C and H, respectively ($n = 9$). * $p < 0.05$. Mean steady-state inactivation curves were obtained for L-type current in control and siTRPC1 (D). $n = 5$. Silencing of $Ca_v1.3$ (E, F) abolished the effect of siTRPC1 on the L-type calcium current. Insets, Western blots from lysates of differentiated SH-SY5Y cells showing decreased expression of TRPC1, $Ca_v1.3$, and STIM1 (as well as overexpression of STIM1 in siSTIM1 cells, rescue) using respective siRNAs. Overexpression of full-length STIM1 in siSTIM1-expressing cells (rescue) showed an increase in Ca^{2+} influx (I, J). K, Average histogram for current density in various conditions. * $p < 0.05$.

munoprecipitation of $Ca_v1.3$ and TRPC1 (Fig. 7F). Importantly, store depletion (+Tg) showed a significant increase in $Ca_v1.3$ -TRPC1-STIM1 interaction (Fig. 7F). Similar results were also obtained using $Ca_v1.3$ antibodies, which showed that $Ca_v1.3$ in-

teracts with STIM1 and TRPC1 and the association between $Ca_v1.3$ -TRPC1-STIM1 was again increased upon Tg treatment (Fig. 7F). We further tested the importance of this association, and cell viability assays were performed. Importantly, TRPC1 or

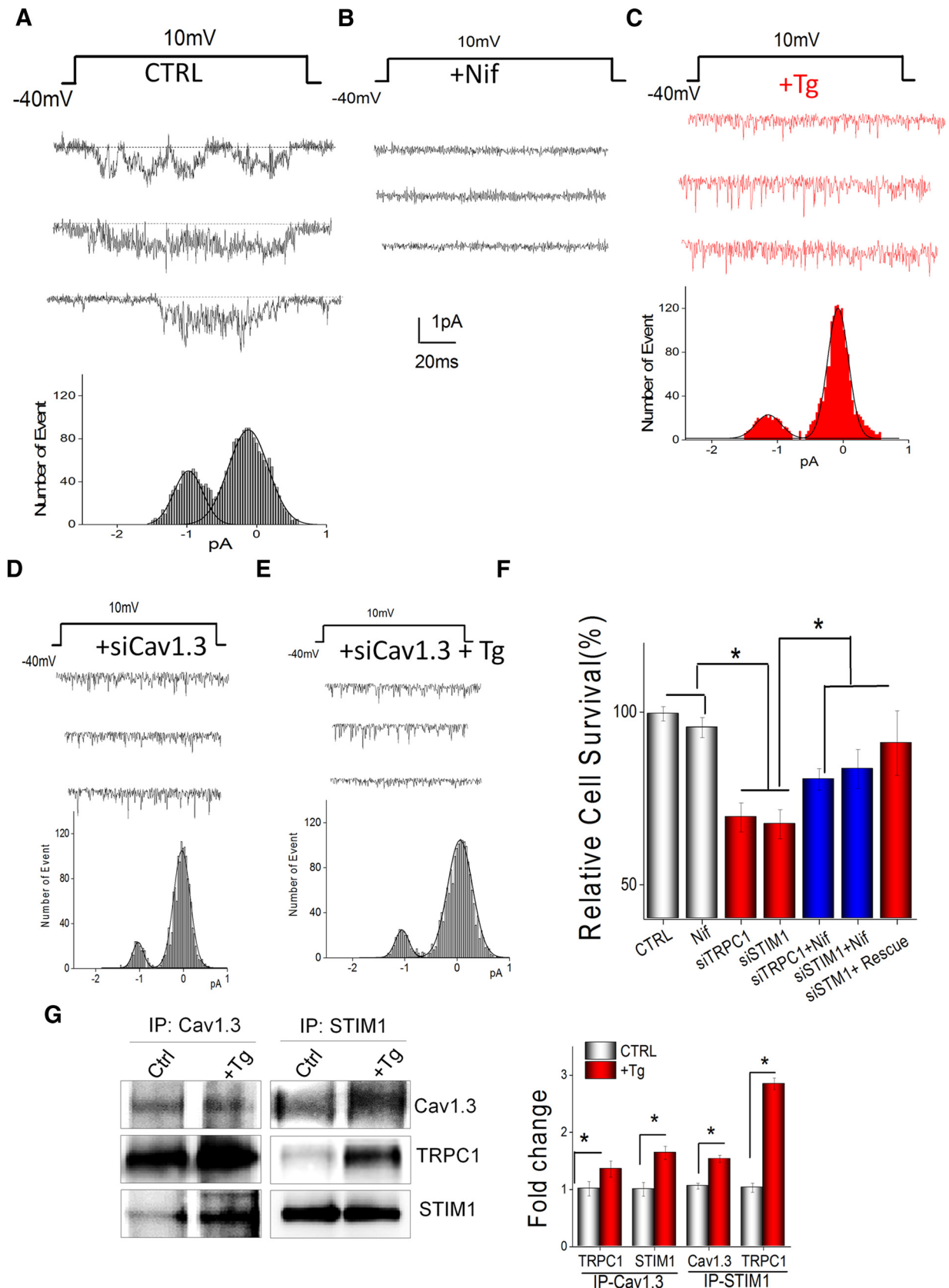


Figure 7. TRPC1 affect $Ca_v1.3$ channels in SH-SY5Y cells. Single-channel recording (from individual differentiated 10–12 SH-SY5Y cells in each condition) using step protocol from -40 mV to 10 mV in control (**A**), nifedipine ($1 \mu\text{M}$) (**B**), Tg-treated ($1 \mu\text{M}$) cells (**C**), and siCav1.3 cells (**D**, **E**). Variance histograms were generated with Gaussian fits and are shown at the bottom of the traces. **F**, Western blots of coimmunoprecipitates of SH-SY5Y cells using $Ca_v1.3$ or STIM1 antibodies in control (CTRL) or stimulated (+Tg) conditions. Antibodies used for Western blots are labeled in the figure. Quantification of the data from 3 to 5 independent experiments is shown. *Significantly different values ($p < 0.05$). $n = 8$. **G**, Cell viability under various conditions in SH-SY5Y cells is shown. *Significantly different from untreated cells ($p < 0.05$). $n = 4$.

STIM1 silencing significantly decreased cell viability that was partially rescued by the addition of nifedipine (Fig. 7G). Furthermore, the rescue of STIM1 (overexpressing STIM1 after STIM1 silencing) was able to restore cell viability (Fig. 7G). Overall, these results suggest that TRPC1 decreases L-type Ca²⁺ currents by providing STIM1 scaffold, and loss of TRPC1-mediated modulation of Ca_v1.3 channels could lead to DA cell death.

TRPC1 regulates Ca_v1.3 function in neurotoxin model of PD

Neurotoxins (such as MPTP/MPP⁺) that mimic Parkinson's disease have been shown to selectively affect the survival of DA neurons. Our previous studies have shown that MPP⁺ treatment specifically decreased TRPC1 activity (Selvaraj et al., 2012), but the mechanism as for why these cells die was not clear. Thus, we performed electrophysiological recordings on SH-SY5Y cells with and without MPP⁺ treatment. As indicated in Figure 5, MPP⁺-treated cells showed an increase in Ca²⁺ currents (Fig. 8A,B). Also, the Tg-mediated inhibition of Ca²⁺ currents was abolished upon MPP⁺ treatment (Fig. 8A,B). Importantly, overexpression of TRPC1 inhibited the MPP⁺-induced increase in L-type calcium currents, suggesting that restoration of TRPC1 expression is essential for the inhibition of L-type calcium currents (Fig. 8A). Notably, siCa_v1.3 also abolished the effects of MPP⁺ and Tg on Ca²⁺ currents, which further suggest that Ca_v1.3 is involved in MPP⁺-facilitated Ca²⁺ currents (Fig. 8C,D). MPP⁺ treatment also showed a decrease in TRPC1 expression without altering STIM1 levels, suggesting a prominent role of TRPC1 in the regulation of Ca_v1.3 currents (Fig. 8E,F). Consistent with these results, the association between Ca_v1.3-TRPC1-STIM1 was decreased in MPP⁺-treated cells (Fig. 8G,H). To further study the role of Ca_v1.3 in neurotoxin models of PD as well as establish the consequence of Ca_v1.3-TRPC1 interactions in PD, we investigated proteins that induce cell death in the MPP⁺/MPTP model. Here we found that pretreatment with nifedipine or siCa_v1.3 significantly decreased caspase 3 activations (as observed by cleaved active caspase) and Bak protein levels in the MPP⁺ model (Fig. 8I). Furthermore, similar results were attained in the MPTP *in vivo* model where subsequent increases in caspase 3, Bak, and Bid apoptotic proteins was observed. Interestingly, overexpression of TRPC1 in the SN region inhibited MPTP-induced increases in apoptotic proteins (Fig. 8J). Finally, pretreatment with nifedipine, siCa_v1.3, or overexpression of TRPC1 partially prevented MPP⁺-induced cell death (Fig. 8K). Together, these data suggest that TRPC1 facilitates STIM1-Ca_v1.3 interactions to suppress Ca_v1.3 activity that inhibits caspase3 activation and decreases apoptosis, thereby protecting DA cells against neurotoxin-mediated insults that lead to PD.

Discussion

Although the mechanisms responsible for the preferential loss of DA neurons in PD have been debated for decades, loss of Ca²⁺ homeostasis could be the most important. Ca²⁺ is crucial for a broad range of neuronal functions, and regulation of intracellular Ca²⁺ concentration represents a major determinant that controls neuronal growth and survival, gene regulation, neuronal excitability, synaptic transmission, and plasticity (Berridge et al., 2000; Sippy et al., 2003; Burgoyne, 2007). Pathological neuronal insults evoke an unwanted rise in cytosolic Ca²⁺ levels, leading to Ca²⁺ overload that causes toxicity and neuronal cell death (Stout et al., 1998; Berridge et al., 2000). VGCCs are multimeric proteins that are essential for the Ca²⁺ influx in neuronal cells. Although several VGCC subunits have been identified, the pore-forming α 1-subunit is the principal determinant for gating and phar-

macology. DA neurons have one of the two α 1-subunits, Ca_v1.2 or Ca_v1.3, that modulate Ca²⁺ influx necessary for their function. In PD, a change has been shown in the ratio of Ca_v1.2 versus Ca_v1.3 that favors a greater utilization of Ca_v1.3 channels, which contributes to the function of DA SN neurons and also seems to render neurons susceptible to excitotoxicity and/or oxidative stress (Henchcliffe and Beal, 2008; Goldberg et al., 2012).

The role of the L-type Ca²⁺ channels in pacemaker activity is still controversial. Previous studies indicate that, in adult DA neurons, the pacemaking activity involves VGCC channels (especially Ca_v1.3) (Nedergaard et al., 1993; Mercuri et al., 1994; Chan et al., 2007; Puopolo et al., 2007; Guzman et al., 2009; Putzier et al., 2009; Drion et al., 2011). In contrast, other studies report the activity of VGCC is not necessary for firing but does contribute to slow oscillatory potentials, which will trigger Na⁺ spikes (Guzman et al., 2009; Dragicevic et al., 2014), suggesting that for the oscillatory phenomenon underlying the pacemaking activity involves a mix of calcium and sodium channels. Although these studies indicate that Ca_v1.3 contributes to pacemaking activity, the mechanism of regulation and whether VGCC is essential for SN DA neurons pacemaker activity remains questionable. Importantly, Ca_v1.3 channels contribute to their progressive loss as observed in PD pathology (Surmeier et al., 2012; Dragicevic et al., 2015). Furthermore, blood-brain barrier-permeable VGCC blockers (e.g., isradipine) protect highly vulnerable DA SN neurons from degeneration in PD and chronic rodent models (Ritz et al., 2010; Ilijic et al., 2011), presumably by reducing Ca²⁺ overload and mitochondrial stress during pacemaking (Guzman et al., 2010; Dragicevic et al., 2015). One possibility for these discrepancies could be that other Ca_v1.3 activity-modulating proteins/channels could be expressed differently. In addition, Ca_v1.3 might cooperate with sodium channels to generate pacemaking with a degree of cooperation that is variable (Drion et al., 2011). Thus, although Ca_v1.3 contributes to the pacemaking activity in DA neurons, it comes with a high metabolic cost. Cytosolic Ca²⁺ levels are tightly controlled, and ATP is needed to sequester Ca²⁺ to inhibit abnormal activation of cells. Thus, dependence on Ca²⁺ for the pacemaking activity could be detrimental for DA neurons. Our results show that, in normal conditions, Ca_v1.3-mediated pacemaking activity is inhibited by TRPC1 thereby protecting DA neurons.

In addition to VGCC, Ca²⁺ release from intracellular ER/SR stores activates Ca²⁺ influx via the SOCE mechanism. The VGCC-mediated Ca²⁺ entry differs from SOCE as VGCCs are activated by depolarization in response to APs, whereas SOCE is activated in response to ER/SR Ca²⁺-store depletion. Notably, both SOCE and VGCC channels are expressed in neurons (Strübing et al., 2001; Selvaraj et al., 2010; Sun et al., 2014); however, the function of SOCE channels in neuronal cells is not well defined. Members of the TRPC and Orai family have been suggested as Ca²⁺ entry channels that regulate SOCE. Additionally, STIM1 has shown to link ER Ca²⁺ store depletion and SOCE activation (Pani et al., 2008, 2012). Upon store depletion, STIM1 aggregates at ER-PM junctions that facilitate its interaction with TRPC1/Orai1 channels, thereby activating SOCE. Importantly, in PD and neurotoxin-treated samples, only TRPC1 expression was altered, whereas no change in Orai1 or STIM1 expression was observed, suggesting that TRPC1 could have a role in PD. Recent studies have also shown that STIM1 strongly suppresses VGCCs (Park et al., 2010; Wang et al., 2010; Harraz and Altier, 2014); however, nothing is known as to whether STIM1 regulates Ca_v1.3 channels and, if so, what mediates this interaction or what is the physiological function of this inhibition. Our results show that, in

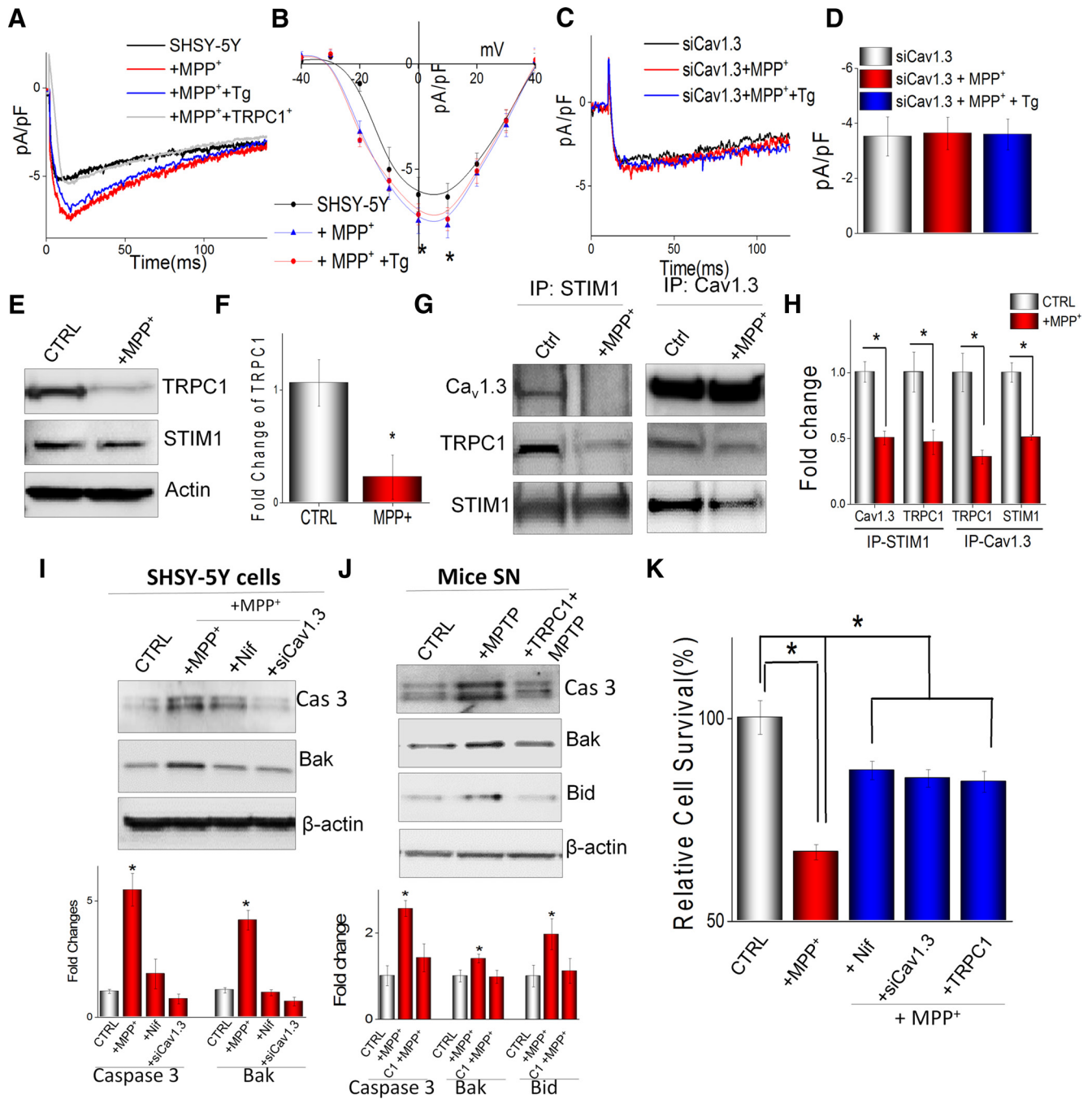


Figure 8. TRPC1 regulates $Ca_v1.3$ function in neurotoxin PD model. **A**, Representative trace showed that calcium currents were evoked in differentiated SH-SY5Y cells with a step protocol from -60 to 10 mV under various conditions. Cells treated with MPP^+ facilitated calcium current, but overexpression of TRPC1 abolished this effect. **B**, $I-V$ curves. **E**, **F**, Western blots of lysates in control and MPP^+ -treated SH-SY5Y cells ($500 \mu M$, 24 h). **C**, **D**, Individual traces of L-type calcium currents in $Ca_v1.3$ silenced cells with and without MPP^+ and/or Tg treatment. **G**, **H**, Coimmunoprecipitates of SH-SY5Y cells using $Ca_v1.3$ and STIM1 antibodies under various conditions. **I**, Western blots of lysates from differentiated SH-SY5Y cells using cleaved caspase3, Bak, and β -actin antibodies under various conditions. **J**, Western blots of lysates from mice SN region using cleaved caspase3, Bak, Bid, and β -actin antibodies under various conditions. For MPTP treatment, mice received MPTP-HCl 25 mg/kg (i.p. for 5 consecutive days at 24 h intervals). Densitometric quantitation for normalized relative to β -actin is shown below the blots. Values are mean \pm SEM from three independent experiments. * $p < 0.05$. **K**, Cell viability under various conditions in SH-SY5Y cells. *Significantly different values from untreated cells ($p < 0.05$). $n = 8$.

DA neurons, STIM1 suppressed $Ca_v1.3$ channels by interacting with $Ca_v1.3$; more importantly, this association was dependent on TRPC1 expression as TRPC1 knock-out mice or TRPC1 silencing showed a significant decrease in store-dependent $Ca_v1.3$ -STIM1 interaction. Moreover, store depletion increased TRPC1-STIM1 interaction and facilitated its association with $Ca_v1.3$ channels, further suggesting that TRPC1 is essential for providing the scaffold necessary for the inhibition of $Ca_v1.3$ channels.

A novel aspect of this study is the documentation of the significance of TRPC1 in regulating L-type Ca^{2+} channel, especially $Ca_v1.3$ function. Our findings reveal that TRPC1 acutely reduced $Ca_v1.3$ currents, which lead to decreased Ca^{2+} entry that could be essential for the inhibition of oxidative stress, thereby increasing the survival of DA neurons. One reason that DA neurons are more vulnerable is the abnormal activation of $Ca_v1.3$ channels, which facilitates sustained elevations in cytosolic Ca^{2+} concen-

tration (Wilson and Callaway, 2000). Increased cytosolic Ca²⁺ could induce mitochondrial dysfunction, and the resulting increase in reactive oxygen species could further advance these DA neurons toward degeneration (Dauer and Przedborski, 2003; Abou-Sleiman et al., 2006; Selvaraj et al., 2010; Sun et al., 2014). In addition to susceptibility to mitochondrial toxins, a decrease in ER Ca²⁺ levels is also known to induce ER stress, which could activate the cell death cascades, as observed in PD (Nguyen et al., 2002; Holtz and O'Malley, 2003; Yoshida et al., 2006; Sun et al., 2014). Importantly, restoration of ER Ca²⁺ stores via TRPC1 activation could protect DA cells against such conditions. Thus, activation of TRPC1 could suppress Ca_v1.3 channels, thus reducing mitochondrial dysfunction and alleviate ER stress to improve DA neurons survival.

Although mechanistic insights regarding how STIM1/TRPC1 may inhibit VGCC needs further investigation, elucidating the relationship between SOCE and VGCC channels in DA neurons could provide insights into the molecular cascade critical for neuronal loss. Herein, our results offer a novel mechanism where TRPC1 regulates Ca_v1.3 channel activity, without altering its inactivation. TRPC1 knock-out mice showed an increase in Ca_v1.3 channel activation and loss of TH-positive neurons, which could be due to increase in the rhythmic activity as nifedipine protected these DA neurons. In addition, TRPC1-mediated inhibition of Ca_v1.3 channels was dependent on STIM1 as STIM1 silencing decreased SOCE and increased Ca_v1.3 activity and loss of TRPC1 abolished STIM1-Ca_v1.3 interaction. Moreover, neurotoxins that mimic PD increased Ca_v1.3 channel activity, and only TRPC1 expression was affected, suggesting that TRPC1 plays an important role in neurotoxin-mediated cell death. Silencing Ca_v1.3 or overexpressing TRPC1 both decreased caspase3 and inhibited MPP⁺-induced cell death. Thus, it could be suggested that TRPC1 expression facilitates STIM1-Ca_v1.3 interactions and is essential for the survival of DA neurons. Although TRPC1 is expressed in most neuronal cells, its loss is only observed in DA neurons in the SN region. Importantly, Ca_v1.3 channels are found at a significantly higher density in DA neurons in the SN region than in the VTA region. Thus, TRPC1-mediated inhibition of Ca_v1.3 channels is specific as it protects DA neurons by reducing the rhythmic activity in the SN region. However, loss of TRPC1 due to the presence of toxins or other insults could abnormally activate Ca_v1.3 channels that would render these neurons vulnerable. In essence, activity-related cellular Ca²⁺ load, mitochondrial dysfunction, as well as oxidative and metabolic stress are particularly important trigger factors for PD (Dragicevic et al., 2015). Moreover, epidemiological studies have shown an association between the use of dihydropyridines (VGCC inhibitors) and decrease the risk for PD (Ritz et al., 2010; Marras et al., 2012), which further suggests that TRPC1 activators could also be a candidate for treating PD patients. Of additional importance is that TRPC1 is also essential for inhibiting ER stress; thus, TRPC1 activation could not only inhibit Ca_v1.3-induced oxidative stress but also inhibit ER stress that together would protect DA neurons from the majority of stressors known to cause PD.

References

- Abou-Sleiman PM, Muqit MM, Wood NW (2006) Expanding insights of mitochondrial dysfunction in Parkinson's disease. *Nat Rev Neurosci* 7:207–219. [CrossRef Medline](#)
- Berridge MJ, Lipp P, Bootman MD (2000) The versatility and universality of calcium signalling. *Nat Rev Mol Cell Biol* 1:11–21. [CrossRef Medline](#)
- Björklund A, Dunnett SB (2007) Dopamine neuron systems in the brain: an update. *Trends Neurosci* 30:194–202. [CrossRef Medline](#)
- Bollimuntha S, Singh BB, Shavali S, Sharma SK, Ebadi M (2005) TRPC1-mediated inhibition of 1-methyl-4-phenylpyridinium ion neurotoxicity in human SH-SY5Y neuroblastoma cells. *J Biol Chem* 280:2132–2140. [CrossRef Medline](#)
- Bollimuntha S, Ebadi M, Singh BB (2006) TRPC1 protects human SH-SY5Y cells against salololol-induced cytotoxicity by inhibiting apoptosis. *Brain Res* 1099:141–149. [CrossRef Medline](#)
- Burgoyne RD (2007) Neuronal calcium sensor proteins: generating diversity in neuronal Ca²⁺ signalling. *Nat Rev Neurosci* 8:182–193. [CrossRef Medline](#)
- Chan CS, Guzman JN, Ilijic E, Mercer JN, Rick C, Tkatch T, Meredith GE, Surmeier DJ (2007) 'Rejuvenation' protects neurons in mouse models of Parkinson's disease. *Nature* 447:1081–1086. [CrossRef Medline](#)
- Dauer W, Przedborski S (2003) Parkinson's disease: mechanisms and models. *Neuron* 39:889–909. [CrossRef Medline](#)
- Dragicevic E, Poetschke C, Duda J, Schlaudraff F, Lammel S, Schiemann J, Fauler M, Hetzel A, Watanabe M, Lujan R, Malenka RC, Striessnig J, Liss B (2014) Cav1.3 channels control D2-autoreceptor responses via NCS-1 in substantia nigra dopamine neurons. *Brain* 137:2287–2302. [CrossRef Medline](#)
- Dragicevic E, Schiemann J, Liss B (2015) Dopamine midbrain neurons in health and Parkinson's disease: emerging roles of voltage-gated calcium channels and ATP-sensitive potassium channels. *Neuroscience* 284:798–814. [CrossRef Medline](#)
- Drion G, Massotte L, Sepulchre R, Seutin V (2011) How modeling can reconcile apparently discrepant experimental results: the case of pacemaking in dopaminergic neurons. *PLoS Comput Biol* 7:e1002050. [CrossRef Medline](#)
- Dryanovski DI, Guzman JN, Xie Z, Galteri DJ, Volpicelli-Daley LA, Lee VM, Miller RJ, Schumacker PT, Surmeier DJ (2013) Calcium entry and alpha-synuclein inclusions elevate dendritic mitochondrial oxidant stress in dopaminergic neurons. *J Neurosci* 33:10154–10164. [CrossRef Medline](#)
- Goldberg JA, Guzman JN, Estep CM, Ilijic E, Kondapalli J, Sanchez-Padilla J, Surmeier DJ (2012) Calcium entry induces mitochondrial oxidant stress in vagal neurons at risk in Parkinson's disease. *Nat Neurosci* 15:1414–1421. [CrossRef Medline](#)
- Guzman JN, Sánchez-Padilla J, Chan CS, Surmeier DJ (2009) Robust pacemaking in substantia nigra dopaminergic neurons. *J Neurosci* 29:11011–11019. [CrossRef Medline](#)
- Guzman JN, Sanchez-Padilla J, Wokosin D, Kondapalli J, Ilijic E, Schumacker PT, Surmeier DJ (2010) Oxidant stress evoked by pacemaking in dopaminergic neurons is attenuated by DJ-1. *Nature* 468:696–700. [CrossRef Medline](#)
- Harraz OF, Altier C (2014) STIM1-mediated bidirectional regulation of Ca(2+) entry through voltage-gated calcium channels (VGCC) and calcium-release activated channels (CRAC). *Front Cell Neurosci* 8:43. [CrossRef Medline](#)
- Helton TD, Xu W, Lipscombe D (2005) Neuronal L-type calcium channels open quickly and are inhibited slowly. *J Neurosci* 25:10247–10251. [CrossRef Medline](#)
- Henchcliffe C, Beal MF (2008) Mitochondrial biology and oxidative stress in Parkinson disease pathogenesis. *Nat Clin Pract Neurol* 4:600–609. [CrossRef Medline](#)
- Holtz WA, O'Malley KL (2003) Parkinsonian mimetics induce aspects of unfolded protein response in death of dopaminergic neurons. *J Biol Chem* 278:19367–19377. [CrossRef Medline](#)
- Huang GN, Zeng W, Kim JY, Yuan JP, Han L, Muallem S, Worley PF (2006) STIM1 carboxyl-terminus activates native SOC, I(crac) and TRPC1 channels. *Nat Cell Biol* 8:1003–1010. [CrossRef Medline](#)
- Hurley MJ, Gentleman SM, Dexter DT (2015) Calcium CaV1 channel subtype mRNA expression in Parkinson's disease examined by in situ hybridization. *J Mol Neurosci* 55:715–724. [CrossRef Medline](#)
- Ilijic E, Guzman JN, Surmeier DJ (2011) The L-type channel antagonist isradipine is neuroprotective in a mouse model of Parkinson's disease. *Neurobiol Dis* 43:364–371. [CrossRef Medline](#)
- Kang S, Cooper G, Dunne SF, Dusel B, Luan CH, Surmeier DJ, Silverman RB (2012) CaV1.3-selective L-type calcium channel antagonists as potential new therapeutics for Parkinson's disease. *Nat Commun* 3:1146. [CrossRef Medline](#)
- Kazuno AA, Munakata K, Nagai T, Shimozono S, Tanaka M, Yoneda M, Kato N, Miyawaki A, Kato T (2006) Identification of mitochondrial DNA

- polymorphisms that alter mitochondrial matrix pH and intracellular calcium dynamics. *PLoS Genet* 2:e128. [CrossRef Medline](#)
- Koschak A, Reimer D, Huber I, Grabner M, Glossmann H, Engel J, Striessnig J (2001) $\alpha 1D$ (Cav1.3) subunits can form I-type Ca²⁺ channels activating at negative voltages. *J Biol Chem* 276:22100–22106. [CrossRef Medline](#)
- Liu X, Singh BB, Ambudkar IS (2003) TRPC1 is required for functional store-operated Ca²⁺ channels: role of acidic amino acid residues in the S5–S6 region. *J Biol Chem* 278:11337–11343. [CrossRef Medline](#)
- Liu X, Cheng KT, Bandyopadhyay BC, Pani B, Dietrich A, Paria BC, Swaim WD, Beech D, Yildirim E, Singh BB, Birnbaumer L, Ambudkar IS (2007) Attenuation of store-operated Ca²⁺ current impairs salivary gland fluid secretion in TRPC1(–/–) mice. *Proc Natl Acad Sci U S A* 104:17542–17547. [CrossRef Medline](#)
- Marcantoni A, Vandaal DH, Mahapatra S, Carabelli V, Sinnegger-Brauns MJ, Striessnig J, Carbone E (2010) Loss of Cav1.3 channels reveals the critical role of L-type and BK channel coupling in pacemaking mouse adrenal chromaffin cells. *J Neurosci* 30:491–504. [CrossRef Medline](#)
- Marras C, Gruneir A, Rochon P, Wang X, Anderson G, Brochie J, Bell CM, Fox S, Austin PC (2012) Dihydropyridine calcium channel blockers and the progression of parkinsonism. *Ann Neurol* 71:362–369. [CrossRef Medline](#)
- Matsuda Y, Fujimura K, Yoshida S (1987) Two types of neurons in the substantia nigra pars compacta studied in a slice preparation. *Neurosci Res* 5:172–179. [CrossRef Medline](#)
- Mercuri NB, Bonci A, Calabresi P, Stratta F, Stefani A, Bernardi G (1994) Effects of dihydropyridine calcium antagonists on rat midbrain dopaminergic neurons. *Br J Pharmacol* 113:831–838. [CrossRef Medline](#)
- Nedergaard S, Flatman JA, Engberg I (1993) Nifedipine- and omega-conotoxin-sensitive Ca²⁺ conductances in guinea-pig substantia nigra pars compacta neurons. *J Physiol* 466:727–747. [CrossRef Medline](#)
- Nguyen HN, Wang C, Perry DC (2002) Depletion of intracellular calcium stores is toxic to SH-SY5Y neuronal cells. *Brain Res* 924:159–166. [CrossRef Medline](#)
- Okamoto T, Harnett MT, Morikawa H (2006) Hyperpolarization-activated cation current (I_h) is an ethanol target in midbrain dopamine neurons of mice. *J Neurophysiol* 95:619–626. [CrossRef Medline](#)
- Pani B, Ong HL, Liu X, Rauser K, Ambudkar IS, Singh BB (2008) Lipid rafts determine clustering of STIM1 in endoplasmic reticulum-plasma membrane junctions and regulation of store-operated Ca²⁺ entry (SOCE). *J Biol Chem* 283:17333–17340. [CrossRef Medline](#)
- Pani B, Bollimuntha S, Singh BB (2012) The TR (i)P to Ca(2)(+) signaling just got STIMy: an update on STIM1 activated TRPC channels. *Front Biosci* 17:805–823. [CrossRef Medline](#)
- Park CY, Shcheglovitov A, Dolmetsch R (2010) The CRAC channel activator STIM1 binds and inhibits L-type voltage-gated calcium channels. *Science* 330:101–105. [CrossRef Medline](#)
- Puopolo M, Raviola E, Bean BP (2007) Roles of subthreshold calcium current and sodium current in spontaneous firing of mouse midbrain dopamine neurons. *J Neurosci* 27:645–656. [CrossRef Medline](#)
- Putzier I, Kullmann PH, Horn JP, Levitan ES (2009) Cav1.3 channel voltage dependence, not Ca²⁺ selectivity, drives pacemaker activity and amplifies bursts in nigral dopamine neurons. *J Neurosci* 29:15414–15419. [CrossRef Medline](#)
- Richards CD, Shiroyama T, Kitai ST (1997) Electrophysiological and immunocytochemical characterization of GABA and dopamine neurons in the substantia nigra of the rat. *Neuroscience* 80:545–557. [CrossRef Medline](#)
- Ritz B, Rhodes SL, Qian L, Schernhammer E, Olsen JH, Friis S (2010) L-type calcium channel blockers and Parkinson disease in Denmark. *Ann Neurol* 67:600–606. [CrossRef Medline](#)
- Selvaraj S, Watt JA, Singh BB (2009) TRPC1 inhibits apoptotic cell degeneration induced by dopaminergic neurotoxin MPTP/MPP(+). *Cell Calcium* 46:209–218. [CrossRef Medline](#)
- Selvaraj S, Sun Y, Singh BB (2010) TRPC channels and their implication in neurological diseases. *CNS Neurol Disord Drug Targets* 9:94–104. [CrossRef Medline](#)
- Selvaraj S, Sun Y, Watt JA, Wang S, Lei S, Birnbaumer L, Singh BB (2012) Neurotoxin-induced ER stress in mouse dopaminergic neurons involves downregulation of TRPC1 and inhibition of AKT/mTOR signaling. *J Clin Invest* 122:1354–1367. [CrossRef Medline](#)
- Seutin V, Engel D (2010) Differences in Na⁺ conductance density and Na⁺ channel functional properties between dopamine and GABA neurons of the rat substantia nigra. *J Neurophysiol* 103:3099–3114. [CrossRef Medline](#)
- Sinnegger-Brauns MJ, Huber IG, Koschak A, Wild C, Obermair GJ, Einzinger U, Hoda JC, Sartori SB, Striessnig J (2009) Expression and 1,4-dihydropyridine-binding properties of brain L-type calcium channel isoforms. *Mol Pharmacol* 75:407–414. [CrossRef Medline](#)
- Sippy T, Cruz-Martín A, Jeromin A, Schweizer FE (2003) Acute changes in short-term plasticity at synapses with elevated levels of neuronal calcium sensor-1. *Nat Neurosci* 6:1031–1038. [CrossRef Medline](#)
- Stout AK, Raphael HM, Kanterewicz BI, Klann E, Reynolds IJ (1998) Glutamate-induced neuron death requires mitochondrial calcium uptake. *Nat Neurosci* 1:366–373. [CrossRef Medline](#)
- Strübing C, Krapivinsky G, Krapivinsky L, Clapham DE (2001) TRPC1 and TRPC5 form a novel cation channel in mammalian brain. *Neuron* 29:645–655. [CrossRef Medline](#)
- Sun Y, Sukumaran P, Bandyopadhyay BC, Singh BB (2014) Physiological function and characterization of TRPCs in neurons. *Cells* 3:455–475. [CrossRef Medline](#)
- Surmeier DJ, Guzman JN, Sanchez-Padilla J, Schumacker PT (2011) The role of calcium and mitochondrial oxidant stress in the loss of substantia nigra pars compacta dopaminergic neurons in Parkinson's disease. *Neuroscience* 198:221–231. [CrossRef Medline](#)
- Surmeier DJ, Guzman JN, Sanchez J, Schumacker PT (2012) Physiological phenotype and vulnerability in Parkinson's disease. *Cold Spring Harb Perspect Med* 2:a009290. [CrossRef Medline](#)
- Vandaal DH, Zuccotti A, Striessnig J, Carbone E (2012) Ca(V)1.3-driven SK channel activation regulates pacemaking and spike frequency adaptation in mouse chromaffin cells. *J Neurosci* 32:16345–16359. [CrossRef Medline](#)
- Wang GX, Poo MM (2005) Requirement of TRPC channels in netrin-1-induced chemotropic turning of nerve growth cones. *Nature* 434:898–904. [CrossRef Medline](#)
- Wang Y, Deng X, Mancarella S, Hendron E, Eguchi S, Soboloff J, Tang XD, Gill DL (2010) The calcium store sensor, STIM1, reciprocally controls Orai and CaV1.2 channels. *Science* 330:105–109. [CrossRef Medline](#)
- Wilson CJ, Callaway JC (2000) Coupled oscillator model of the dopaminergic neuron of the substantia nigra. *J Neurophysiol* 83:3084–3100. [CrossRef Medline](#)
- Xu W, Lipscombe D (2001) Neuronal Ca(V)1.3 α (1) L-type channels activate at relatively hyperpolarized membrane potentials and are completely inhibited by dihydropyridines. *J Neurosci* 21:5944–5951. [CrossRef Medline](#)
- Yoshida I, Monji A, Tashiro K, Nakamura K, Inoue R, Kanba S (2006) Depletion of intracellular Ca²⁺ store itself may be a major factor in thapsigargin-induced ER stress and apoptosis in PC12 cells. *Neurochem Int* 48:696–702. [CrossRef Medline](#)
- Yung WH, Häusser MA, Jack JJ (1991) Electrophysiology of dopaminergic and non-dopaminergic neurons of the guinea-pig substantia nigra pars compacta in vitro. *J Physiol* 436:643–667. [CrossRef Medline](#)
- Zhang HP, Xiao Z, Cilz NI, Hu B, Dong H, Lei S (2014) Bombesin facilitates GABAergic transmission and depresses epileptiform activity in the entorhinal cortex. *Hippocampus* 24:21–31. [CrossRef Medline](#)